Research Square

Preprints are preliminary reports that have not undergone peer review.
They should not be considered conclusive, used to inform clinical practice,
or referenced by the media as validated information.

How Green nano zero valent iron compares to Industrial Iron nanoparticles in Driving Sustainable Hydrocarbon Bioremediation

Yakubu Yakmut Saleh

yakubu.saleh@strath.ac.uk

University of Strathclyde

Charles Knapp

University of Strathclyde

Akinseye Olanrewaju

University of Strathclyde

Research Article

Keywords: Green nZVI, Microbial community dynamics, Hydrocarbon-degrading bacteria, Ring-hydroxylating dioxygenases, Nanobioremediation, Operational Taxonomic Units

Posted Date: April 1st, 2026

DOI: https://doi.org/10.21203/rs.3.rs-8949593/v1

License: This work is licensed under a Creative Commons Attribution 4.0 International License.
Read Full License

Additional Declarations: No competing interests reported.

Title

How Green nano zero valent iron compares to Industrial Iron nanoparticles in Driving Sustainable Hydrocarbon Bioremediation.

Author Information

Name of Authors: Yakubu Yakmut Saleh*, Charles W. Knapp, Akinseye Olanrewaju

ORCiD of Author: 0009-0000-8766-6494

Affiliation: Department of Civil and Environmental Engineering, University of Strathclyde, Glasgow, United Kingdom G1 1XJ

Corresponding Email: yakubu.saleh@strath.ac.uk

Abstract

Green nano-zero-valent iron (nZVI) has been promoted as an eco-friendlier alternative to industrial and chemically synthesised nZVI, yet direct comparisons of their chemical and biological performance remain scarce. This study evaluated both formulations in 100 ml microcosms containing diesel-contaminated freshwater. Triplicate batches received 0.004 mg/L, 0.01 mg/L, and 0.02 mg/L of either green nZVI (18.6 mg/L) or commercial nZVI (20 mg/L); untreated flasks served as controls. Chemical oxygen demand (COD) and gas chromatography–flame-ionisation detection (GC-FID) tracked total petroleum hydrocarbons (TPH) at two hours and 24 hours, while 16S-rRNA amplicon sequencing profiled microbial communities.

Industrial nZVI delivered the fastest abiotic removal, cutting COD from 179 mg/l to 20 mg/l and TPH from 58 mg/l to 16 mg/l, reflecting a 73 % reduction within 24 hours at 0.02 mg/L dosage. However, reactive-oxygen bursts depressed microbial abundance by approximately 25% relative to the 9,510 Operational Taxonomic Units (OTU) control. Green nZVI achieved slightly lower 24-hour removals (COD 49–68 %; TPH 56–64 %), but tripled biomass to 34,000 OTUs and selectively enriched hydrocarbon-degrading taxa, including *Betaproteobacteria* and *Actinobacteria*. Statistical tests confirmed a non-significant population decline for industrial nZVI ($t = -2.52$, $p = 0.053$) and a significant rise for green nZVI ($t = 3.89$, $p = 0.012$). Optimum performance occurred at the lowest green dose of 0.004 mg/L for both green and industrial nZVI, where TPH fell by 73% for Industrial nZVI and 64% for green nZVI, while the community expanded three-fold, bolstering synergistic nano-bio interactions.

These findings demonstrate that plant-derived nZVI can rival industrial particles in hydrocarbon removal while enhancing microbial resilience, furnishing dose windows, contact-time targets, and monitoring benchmarks for sustainable nanobioremediation.

Keywords

Green nZVI, Microbial community dynamics, Hydrocarbon-degrading bacteria, Ring-hydroxylating dioxygenases, Nanobioremediation, Operational Taxonomic Units.

1 Introduction

Hydrocarbon ingress into aquatic systems driven by oil-field discharges, transport spills, industrial effluents and urban runoff poses chronic threats to water quality, ecosystem integrity and human health because these hydrophobic compounds accumulate in sediments and bio-magnify across food webs (Aliyar Zanjani et al., 2015, Alegbeleye et al., 2017, Abdel-Shafy and Mansour, 2019). Conventional clean-up measures, including excavation, sorbents, surfactant washing, chemical oxidation, and nutrient-boosted biostimulation, can be successful in niche settings but often struggle with recalcitrant fractions such as BTEX and high-molecular-weight PAHs, which generate secondary wastes or prove cost-intensive at scale (Chang et al., 2005, Bradl and Xenidis, 2005, Dhaka and Chattopadhyay, 2021). Consequently, there is an urgent need for remediation technologies that combine rapid contaminant removal with long-term ecological compatibility.

Nanotechnology has emerged as a promising bridge between these competing demands. In particular, nanoscale zero-valent iron (nZVI) offers exceptionally high surface area and redox reactivity that enable both reductive dechlorination of chlorinated ethenes and Fenton-like oxidative mineralisation of aromatic hydrocarbons (Arun Gavaskar, 2005, Crane and Scott, 2012). Chemically and industrially produced nZVI rapidly eliminates dissolved pollutants but is prone to aggregation, passivation and potential eco-toxicity (Barzan et al., 2014, Bhat et al., 2023). Green-synthesised nZVI, reduced by plant polyphenols or microbial metabolites, retains comparable reactivity while its organic capping layers mitigate oxidation, increase colloidal stability and markedly lower toxicity risks, making it attractive for field deployment in resource-constrained regions(Devatha et al., 2016, Ebrahiminezhad et al., 2018, Fahmy et al., 2018).

Biological degradation remains nature's most complete polishing step. Specialist hydrocarbonoclastic bacteria such as *Pseudomonas*, *Alcanivorax*, *Rhodococcus* and sulfate-reducing *Desulfovibrio* catabolise alkanes, BTEX and PAHs via oxygenase-mediated pathways (Abbasian et al., 2015, Coenye, 2013, Gutierrez, 2019), while white-rot fungi (*Phanerochaete chrysosporium*, *Trametes versicolor*) and algal genera (*Chlorella*, *Scenedesmus*) contribute complementary metabolic routes (Macaya et al., 2019, Oladipo et al., 2025). Expression of ring-hydroxylating dioxygenase (RHD) genes underpins many of these transformations, enabling cleavage of otherwise recalcitrant aromatic rings (Paisse et al., 2011, Martin et al., 2013, Chemerys et al., 2014). Yet native microbial communities in heavily oiled

waters are frequently suppressed by toxicity, low oxygen or nutrient limitations, curtailing natural attenuation rates (Khan et al., 2018).

The convergence of nanotechnology and microbiology, termed “nanobioremediation”, seeks to harness nZVI’s abiotic oxidation–reduction power to unlock or accelerate subsequent biotic mineralisation (Bhatt et al., 2022, Gul et al., 2022, Miranda et al., 2022). Studies have shown that iron nanoparticles can fragment high-molecular-weight hydrocarbons into smaller, more bioavailable intermediates, donate electrons to iron-reducing consortia, and, when dosed judiciously, stimulate rather than inhibit community diversity (Hajipour et al., 2012, Hamdy et al., 2021). Green nZVI is particularly suited to this role because its slow iron release and benign capping agents ease oxidative stress, fostering cooperative rather than antagonistic nano-bio interactions (Rebello et al., 2021, Banerjee et al., 2022).

Knowledge on how different nZVI formulations sculpt native hydrocarbon-degrading communities remains sparse. Here, identified oil-impacted freshwater microcosms are exposed to graded doses of green-synthesised versus industrial nZVI and their profiles are tracked over time. These coupled chemical–ecological data identify dose windows that maximise nano-bio synergy and underline the sustainability advantages of polyphenol-capped iron nanoparticles.

2 Materials and Methods

2.1 Water sample collection and preliminary tests

Contaminated water samples were extracted from soils at a former maintenance shipyard near Clydebank, along the River Clyde, near Glasgow. The soils were exhumed 1-2 metres below the surface. As the soil was removed, an oily sheen was observed in the pooled water. The porewater was extracted, the oil was decanted, and the contaminated water was collected and diluted with more Clyde River water. The sample was tested for pH and conductivity using a Thermo Scientific Orion Star A215 pH/Conductivity meter.

2.2 Synthesising Green nano zero-valent iron

Dried green tea leaves used for the synthesis of green nZVI were obtained as a commercially packaged food-grade product purchased from Lidl supermarket. The product was a Polish-import green tea packaged in Dublin, Ireland, and sold as dried Camellia sinensis leaves in tea bags. It was purchased in Glasgow, Scotland, in 2024 and used without further purification for the preparation of the plant extract. Because the material was commercially sourced, the original cultivation location of the tea leaves could not be determined beyond the manufacturer’s labelling.

10g of dried green tea leaves were steeped in 100 ml of de-ionised water in a 250 ml round-bottom flask, maintained at 70 °C on a magnetic stirrer for 1 hour. The hot suspension was then passed

through a 0.22 µm membrane to yield a clear polyphenol extract. A 0.1 M $FeCl_3 \cdot 6H_2O$ stock was prepared by dissolving 5.4 g of iron (III) chloride hexahydrate (99 %+, Fisher Scientific, Loughborough, UK) in 200 mL of de-ionised water. To generate green-synthesised nZVI, 200 ml of this ferric solution was titrated with 100 mL of the filtered green-tea extract (ratio 2:1). The mixture instantaneously turned black, evidence of nanoparticle formation, yet remained acidic, so 2.5 mL of 10M NaOH (Merck Sigma-Aldrich) was added to stabilise the pH at 6.5–7.5. The suspension was centrifuged in an Eppendorf 5804 R (10,000rpm/9950rcf/1047.2 rad/s for 5 min), the supernatant decanted, and the pellet washed twice with de-ionised water and once with isopropanol (99.5 %, HPLC grade, Fisher Chemical, Loughborough, UK) and centrifuged again before decanting to keep a slurry mixture. The entire synthesis process was performed in the Environmental Chemistry Laboratory of the Department of Civil and Environmental Engineering at the University of Strathclyde, Glasgow.

2.3 Cultivation of Indigenous Bacteria

The indigenous microbial community in the river water sample was enriched with a broth mixture containing di-potassium phosphate (14 g/L), mono-potassium phosphate (4 g/L), sodium citrate (1 g/L), magnesium sulphate (0.2 g/L), and ammonium sulphate (2 g/L) in 1 L of deionised water. The broth mixture was added to the contaminated water to promote bacterial growth and allowed to culture at a room temperature of 20°C for four (4) weeks.

2.4 Batch Sampling and Dosing Regime

The cultured contaminated water batch samples (100 ml each) were established in sterile 250 ml conical flasks and held at room temperature (20°C). Two zerovalent-iron formulations were evaluated: Green nZVI synthesised in-house (18.6 mg/L concentration) as described in Section 2.2, and Industrial nZVI powder (35–45 nm particle size, 99.5% trace metal basis; Sigma-Aldrich, Steinheim, Germany) diluted to 20 mg/L concentration in de-ionised water. Each stock was vortexed immediately before use to minimise settling. Doses of 0.004mg/L, 0.01mg/L, and 0.02mg/L were pipetted into separate flasks. Triplicate flasks were prepared for each dose-formulation combination. Flasks were orbitally shaken (120 rpm) to keep particles suspended to avoid aggregation.

2.5 Measuring Hydrocarbon Degradation

Chemical oxygen demand (COD) was used as a rapid proxy for bulk hydrocarbon load. 2ml of each treated or control batch (0.004, 0.01 or 0.02 mg/L green or industrial nZVI; 2 hours and 24 hours) were digested in HACH LCK 400 cuvettes (148°C for 2 hours) and read at 605 nm on a DR6000 UV-Vis spectrophotometer, yielding COD values in mg/L for direct comparison of removal efficiencies.

For compound-specific resolution, hydrocarbons were recovered by triplicate dichloromethane liquid-liquid extraction (USEPA 3510C), concentrated to 1 mL and analysed on a Thermo Finnigan Focus Gas Chromatograph with Flame Ionisation Detection (GC-FID). Instrument calibration (10–100 ppm Florida TRPH mix) enabled quantification of total petroleum hydrocarbons (TPH) in each sample. Overlaid chromatograms (3–45 min window) illustrated peak suppression relative to the untreated baseline, linking dose and formulation to TPH abatement. Together, the COD figures and GC-FID fingerprints provided complementary metrics of nano-iron-driven hydrocarbon degradation.

2.6 DNA extraction and 16S rRNA amplicon sequencing

Microbial DNA was recovered from each 100 ml batch sample by filtering the entire volume onto 0.22µm membranes and processing the filters with an MP FastDNA™ Spin Kit (MP Biomedicals, USA). Filters were aseptically transferred to lysing-matrix tubes, mixed with MT-Buffer and sodium-phosphate buffer, and bead-beaten in a FastPrep-24 (6 m/s for 40s). After centrifugation, the supernatant was clarified with Protein Precipitation Solution, the DNA was bound to the kit's silica-clay matrix, washed with SEWS-M, and finally eluted in 100 µl nuclease-free water. Eluates were stored at –80°C until analysis.

Purity and yield were confirmed on a BioTek Gen5 micro-volume spectrophotometer (2 µl per sample). Blank (DES water) readings were run first, followed by the extracts; OD_{260}, OD_{280} and OD_{320} were recorded, and only samples with $OD_{260}/_{280} \geq 1.8$ were advanced to sequencing.

100µl volumes of each qualified extract were shipped on dry ice to the NU'Omics sequencing facility (Northumbria University, UK). NU'Omics performed PCR amplification of the bacterial 16S rRNA V4 region and the fungal ITS-2 region, library preparation and paired-end (2 × 250 bp) sequencing on an Illumina MiSeq. Raw reads were processed using Quantitative Insights into Microbial Ecology (QIIME) as described by Caporaso et al. (2010) through quality trimming, chimera removal with ChimeraSlayer, clustering into operational taxonomic units (OTUs) at 97 % similarity with the UCLUST algorithm, alignment with PyNAST, and taxonomic assignment against the Green genes database (Caporaso et al., 2012). The resulting OTU tables were exported to Microsoft Excel for downstream quantitative and statistical analyses, linking community shifts to nZVI dose, formulation, and exposure time.

2.7 Bioinformatics and Statistics

The raw taxonomic tables were cleaned in Excel and Python. Only the number columns were kept, empty cells were filled with zeros, and all values were scaled to the same range so they could be compared fairly. Using simple text-search rules, the phylum tag and the order tag were extracted from each taxonomy string. Counts were converted to percentages for every sample, then averaged to find

the ten most common phyla and orders. These results were illustrated in bar charts that give a quick picture of which groups dominate the community.

Extra details hidden in the "DESCRIPTION" column showed which sample got which treatment, at what dose (0.004, 0.01 and 0.02 mg/L per 100 ml) and for how long (2 hours or 24 hours). Using these labels, two t-tests were calculated: one compared each nZVI treatment with the untreated control; the other compared industrial nZVI with green nZVI. The test statistics (t-values and p-values) would determine whether any increase or decrease in OTUs is real or due to chance.

Finally, QIIME2-generated bar charts were reorganised into matched green-versus-industrial frames for every dose–time combination. Overlaying the top 10 taxa per sample exposed formulation-specific and temporal trends. These visualisations, integrated with the statistical outputs, underpinned the experiment's evaluation of nano-bio synergy and sustainable remediation potential.

3 Results

3.1 COD and TPH Removal Performance

Results from the COD tests, summarised in Table 1, showed a clear dose-response: raising the nZVI dose from 0.004mg/L to 0.02mg/L steadily pushed COD lower in every case, with the 0.02mg/L industrial formulation cutting COD from the control's 179 mg/l to 59.1 mg/l after 2 hours and further to 19.8 mg/l after 24 hours. Green nZVI followed the same pattern, moderate drops at 2 hours and much steeper declines by 24 hours. Though its best performance never matched the industrial nZVI at the same dose, the moderate reductions seen at low doses became far larger after 24 hours. Even so, every nZVI treatment outperformed the untreated water.

Table 1: Summary of results from COD tests conducted on treated contaminated water samples

SAMPLES	Industrial nZVI (20 mg/L)		Green nZVI (18.6 mg/L)	
	After 2 Hrs	After 24 Hrs	After 2 Hrs	After 24 Hrs
	COD (mg/L)		COD (mg/L)	
Contaminated Water (CW)	179	172	179	172
CW + 0.004mg/L of nZVI	112.3	67.1	136.4	88.2
CW + 0.01 mg/L of nZVI	214	21.6	144.9	56
CW + 0.02 mg/L of nZVI	59.1	19.8	90.5	31.7

GC-FID overlays and the accompanying Table 2 tell a consistent story: every nZVI dose attenuated the diesel-range peaks (retention 19–33 min) relative to the baseline trace, and the depth of attenuation tracked both dose and contact time. Quantitatively, baseline TPH averaged 58 mg/l; after 24 hours,

the 0.02 mg/L industrial treatment drove that down to 15.7 mg/l (approx. 73% removal), while 0.004 mg/L and 0.004 mg/L yielded 20.9 mg/l (64%) and 19.2 mg/l (67%), respectively. Green nZVI followed the same rank order but with slightly higher residuals: 0.02 mg/L, 0.01 mg/L and 0.004 mg/L left 25.1mg/l, 24.2mg/l and 21.0 mg/l, corresponding to 56%, 58% and 64% removal. Two-hour snapshots captured only partial abatement. For example, a sample treated with 0.10 ml of industrial nZVI lowered TPH to 25.8 mg/L, confirming that most reactivity occurs between 2 hours and 24 hours. Replicate standard deviations (≤ 5 % of the mean) show the patterns are reproducible. Together, the results demonstrate a clear dose and time-dependent advantage for industrial nZVI; it also verifies that even the lowest green nZVI dose achieves > 60 % TPH reduction, underscoring its promise as a more sustainable option.

Table 2 TPH values of treated contaminated water with different doses of industrial and green nZVI.

GC-FID TAG Sample ID	Sample Type	TPH (C8-C40) (mg/L)	Average TPH (mg/L)	Standard Deviation	Average removal efficiency (%)
TPH_CW_1a	Contaminated Water	93.10	58.13	30.41	0.00
TPH_CW_1b	Contaminated Water	37.90			
TPH_CW_1c	Contaminated Water	43.40			
TPH_CW_2a	Contaminated Water + 0.004mg/L of Industrial nZVI after 2 hours	20.68	19.23	1.38	66.92
TPH_CW_2b	Contaminated Water + 0.004mg/L of Industrial nZVI after 2 hours	19.08			
TPH_CW_2c	Contaminated Water + 0.004mg/L of Industrial nZVI after 2 hours	17.93			
TPH_CW_3a	Contaminated Water + 0.01mg/L of Industrial nZVI after 2 hours	22.53	22.61	0.32	61.11
TPH_CW_3b	Contaminated Water + 0.01mg/L of Industrial nZVI after 2 hours	22.96			
TPH_CW_3c	Contaminated Water + 0.01mg/L of Industrial nZVI after 2 hours	22.34			
TPH_CW_4a	Contaminated Water + 0.02mg/L of Industrial nZVI after 2 hours	28.70	25.83	2.67	55.56
TPH_CW_4b	Contaminated Water + 0.02mg/L of Industrial nZVI after 2 hours	23.41			
TPH_CW_4c	Contaminated Water + 0.02mg/L of Industrial nZVI after 2 hours	25.39			
TPH_CW_5a	Contaminated Water + 0.004mg/L of Industrial nZVI after 24 hours	12.10	15.74	3.19	72.92
TPH_CW_5b	Contaminated Water + 0.004mg/L of Industrial nZVI after 24 hours	17.04			
TPH_CW_5c	Contaminated Water + 0.004mg/L of Industrial nZVI after 24 hours	18.08			
TPH_CW_6a	Contaminated Water + 0.01mg/L of Industrial nZVI after 24 hours	17.07	20.92	3.35	64.01
TPH_CW_6b	Contaminated Water + 0.01mg/L of Industrial nZVI after 24 hours	22.70			
TPH_CW_6c	Contaminated Water + 0.01mg/L of Industrial nZVI after 24 hours	23.01			
TPH_CW_7a	Contaminated Water + 0.02mg/L of Industrial nZVI after 24 hours	17.65	19.66	2.72	66.18
TPH_CW_7b	Contaminated Water + 0.02mg/L of Industrial nZVI after 24 hours	22.75			
TPH_CW_7c	Contaminated Water + 0.02mg/L of Industrial nZVI after 24 hours	18.58			
TPH_CW_8a	Contaminated Water + 0.004mg/L of Green nZVI after 2 hours	30.77	31.81	1.26	45.27
TPH_CW_8b	Contaminated Water + 0.004mg/L of Green nZVI after 2 hours	31.46			
TPH_CW_8c	Contaminated Water + 0.004mg/L of Green nZVI after 2 hours	33.22			
TPH_CW_9a	Contaminated Water + 0.01mg/L of Green nZVI after 2 hours	35.38	36.64	1.15	36.97
TPH_CW_9b	Contaminated Water + 0.01mg/L of Green nZVI after 2 hours	36.90			

TPH_CW_9c	Contaminated Water + 0.01mg/L of Green nZVI after 2 hours	37.64			
TPH_CW_10a	Contaminated Water + 0.02mg/L of Green nZVI after 2 hours	34.80	35.32	0.46	39.24
TPH_CW_10b	Contaminated Water + 0.02mg/L of Green nZVI after 2 hours	35.67			
TPH_CW_10c	Contaminated Water + 0.02mg/L of Green nZVI after 2 hours	35.50			
TPH_CW_11a	Contaminated Water + 0.004mg/L of Green nZVI after 24 hours	20.29	20.98	0.94	63.90
TPH_CW_11b	Contaminated Water + 0.004mg/L of Green nZVI after 24 hours	22.06			
TPH_CW_11c	Contaminated Water + 0.004mg/L of Green nZVI after 24 hours	20.60			
TPH_CW_12a	Contaminated Water + 0.01mg/L of Green nZVI after 24 hours	25.16	24.21	0.83	58.35
TPH_CW_12b	Contaminated Water + 0.01mg/L of Green nZVI after 24 hours	23.66			
TPH_CW_12c	Contaminated Water + 0.01mg/L of Green nZVI after 24 hours	23.81			
TPH_CW_13a	Contaminated Water + 0.02mg/L of Green nZVI after 24 hours	27.19	25.05	2.64	56.92
TPH_CW_13b	Contaminated Water + 0.02mg/L of Green nZVI after 24 hours	22.09			
TPH_CW_13c	Contaminated Water + 0.02mg/L of Green nZVI after 24 hours	25.86			

3.2 Taxonomic Composition

Raw microbial reads were first inspected in QIIME2 View (.qzv format) to visualise unfiltered relative abundances as shown in Figure 1. After quality-control filtering, removal of ambiguous, null and ultra-rare features, the taxa were reorganised hierarchically from phylum to order, producing the cleaned dataset summarised in Table 1. This curated list, cross-checked against the hydrocarbon-bioremediation literature, identifies the orders most frequently associated with petroleum degradation, thereby bridging community composition with functional potential for contaminant breakdown.

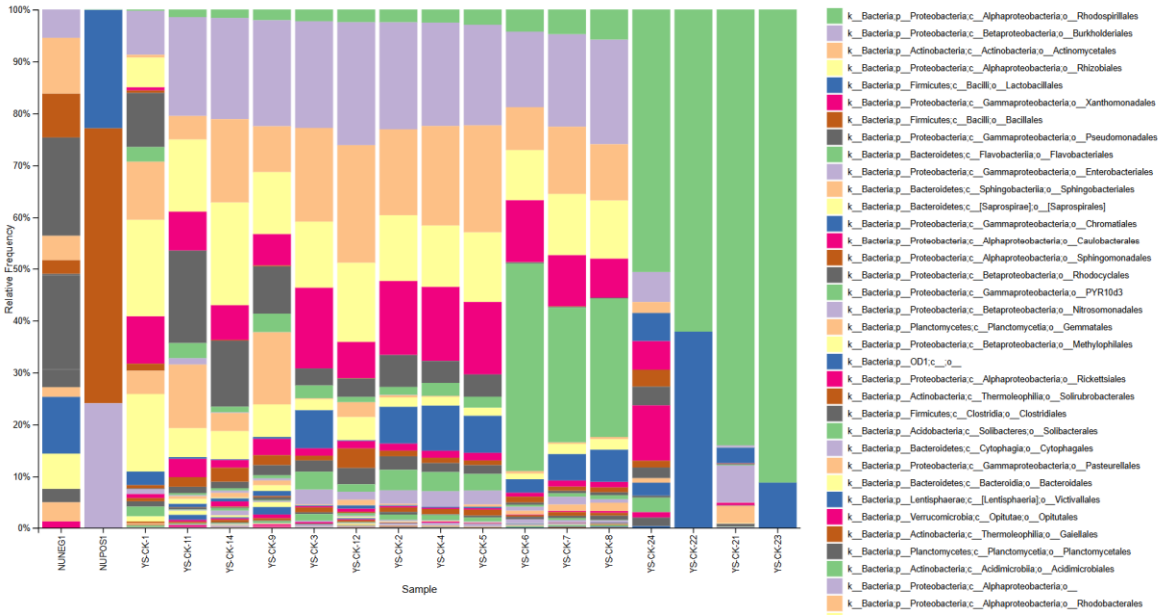


Fig.1: Stacked Bar Chart showing Microbial Community Composition Under Different nZVI Treatments after data clean-up

Table 3 organises the recovered microbiome in a phylum-to-order hierarchy, highlighting in bold the lineages previously classified as hydrocarbonoclastic bacteria (HCBs). All of these groups have been repeatedly detected at oil-impacted sites and are noted for encoding ring-hydroxylating dioxygenases (RHDs) that catalyse the first step of hydrocarbon mineralisation(Phale et al., 2007, Xu et al., 2018, Miller et al., 2019).

Table 3: A summary of the identified bacterial taxa from the QIIME 2 dataset, categorising each order under its respective phylum, class and orders

S/No	Phylum	Class	Representative Orders
1	***Euryarchaeota***	***Halobacteria***	***Halobacteriales***
		Methanomicrobia	*Methanosarcinales*
2	***Acidobacteria***	*Solibacteres*	*Solibacterales*
3	***Actinobacteria***	*Acidimicrobiia*	*Acidimicrobiales*
		Coriobacteriia	*Coriobacteriales*
		Thermoleophilia	
		***Actinobacteria* (Class)**	***Actinomycetales*, *Bifidobacteriales*** (some references subsume these under "Actinomycetia")
4	***Armatimonadetes***	*Fimbriimonadia*	*Fimbriimonadales*
5	***Bacteroidetes***	*Saprospirae*	*Saprospirales*
		Bacteroidia	*Bacteroidales*
		Cytophagia	***Cytophagales***
		Flavobacteriia	***Flavobacteriales***
		Sphingobacteriia	***Sphingobacteriales***
6	***Chloroflexi***	*Anaerolineae*	*Anaerolineales*
		Thermomicrobia	*Thermomicrobiales*
7	***Firmicutes***	*Bacilli*	*Bacillales, Lactobacillales*
		Clostridia	*Clostridiales*
8	***Fusobacteria***	*Fusobacteriia*	*Fusobacteriales*
9	***Gemmatimonadetes***	*Gemmatimonadetes* (Class)	*Gemmatimonadales*
10	***Lentisphaerae***	*Victivallia* (less common)	*Victivallales*
11	***Planctomycetes***	***Planctomycetia***	***Planctomycetales*, *Gemmatales***
12	***Proteobacteria***	***Alphaproteobacteria***	***Rhodobacterales*, *Rhodospirillales, Rickettsiales*, *Sphingomonadales***
		Betaproteobacteria	***Burkholderiales*, *Hydrogenophilales, Methylophilales, Neisseriales, Nitrosomonadales*, *Rhodocyclales***
		Deltaproteobacteria	*Bdellovibrionales*, ***Desulfovibrionales, Desulfuromonadales*, *Myxococcales***
		Gammaproteobacteria	*Aeromonadales, Alteromonadales, Chromatiales, Enterobacteriales, Legionellales*, ***Oceanospirillales***, *Pasteurellales*, ***Pseudomonadales, Xanthomonadales***
13	***Verrucomicrobia***	*Methylacidiphilae* (Class)	*Methylacidiphilales*

		Opitutae	*Opitutales*
		Pedosphaerae (sometimes part of *Verrucomicrobiae or Opitutae)*	*Pedosphaerales*
		Chthoniobacterales (variously placed)	May also appear under *Verrucomicrobiae subgroups*
		Verrucomicrobiales	

Data on the top 10 dominant phyla by OTUs reveal that *Proteobacteria* dominate the community, accounting for 64.04%, with Bacteroidetes (18.25%) and Actinobacteria (14.22%) trailing significantly in second and third place, respectively. While the Order-level data shows *Burkholderiales* lead at 18.67%, followed by *Actinomycetales* (13.24%) and *Rhizobiales* (12.58%).

3.3 Microbial Community Response to Treatment Using nZVI

Table 4 captures the total microbial counts in Operational Taxonomic Units as extracted from QIIME alongside the floating bar charts, summarising how total OTU counts shift with increasing nZVI dose (0.004–0.02 mg/L) and exposure time (2 hours to 24 hours), offering a side-by-side view of dose- and time-dependent microbial responses.

Table 4: Summary of the total microbial count (Operational Taxonomic Units)

DESCRIPTION	MICROBIAL COUNT in OTUs
BLANK Contaminated water sample	9,510
Contaminated water + 0.004mg/L of InZVI after 2 hrs	9,318
Contaminated water + 0.01mg/L of InZVI after 2 hrs	8,854
Contaminated water + 0.02mg/L of InZVI after 2 hrs	9,578
Contaminated water + 0.004mg/L of InZVI after 24 hrs	6,453
Contaminated water + 0.01mg/L of InZVI after 24 hrs	7,727
Contaminated water + 0.02mg/L of InZVI after 24hrs	7,889
Contaminated water + 0.004mg/L of GnZVI after 2 hrs	11,599
Contaminated water + 0.01mg/L of GnZVI after 2 hrs	18,237
Contaminated water + 0.02mg/L of GnZVI after 2 hrs	20,949
Contaminated water + 0.004mg/L of GnZVI after 24 hrs	36,851
Contaminated water + 0.01mg/L of GnZVI after 24 hrs	34,725
Contaminated water + 0.02mg/L of GnZVI after 24 hrs	30,917

Industrial nZVI left microbial counts barely changed after two hours (≈ 8,800–9,600 vs. 9,510 in the control) but drove them down to 6,453–7,889 after 24 hours, an inhibition consistent with uncapped Fe^{o} toxicity and Reactive Oxygen Species (ROS) formation. On the other hand, green nZVI produced the opposite trend: populations jumped to 11,600–20,900 within two hours and soared to 30,917–36,851 by 24 hours, with the 0.004 mg/L dose (36,851) outperforming the 0.02 mg/L dose (30,917). These data suggest that modest, polyphenol-stabilised iron additions create the most favourable

conditions for microbial proliferation, while higher green-nZVI loads and all industrial formulations are less supportive.

T-tests show that industrial nZVI produced only a borderline effect on total microbial counts (t = –2.519 and p = 0.053), whereas green nZVI caused a clear, statistically significant shift relative to the control (t = 3.889 and p = 0.012). A direct comparison of the two formulations revealed an even stronger divergence (t = –4.154, p = 0.002), confirming that green-synthesised iron nanoparticles influence microbial communities very differently from their industrial counterparts and emphasising the importance of formulation choice in nano-bioremediation strategies.

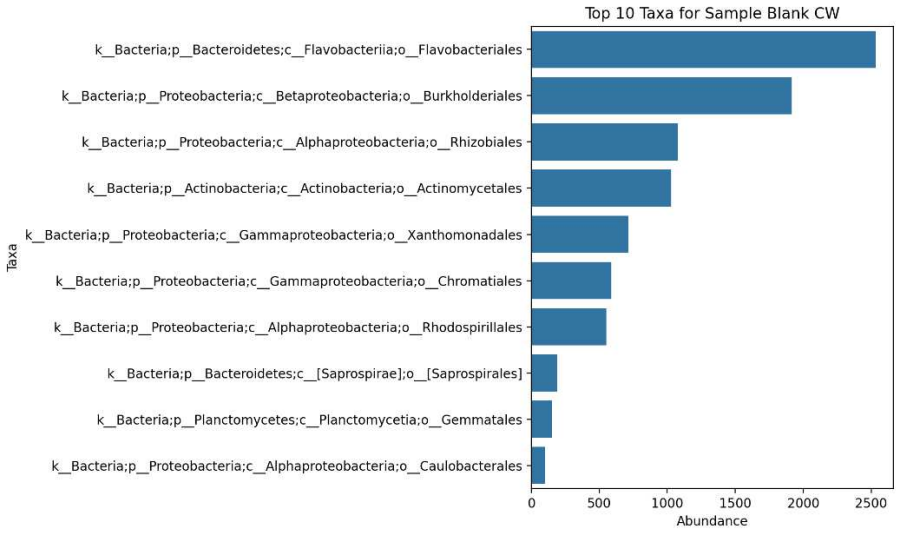


Fig. 2a: Bar chart illustrating the top 10 bacteria (in OTUs) found in untreated contaminated water

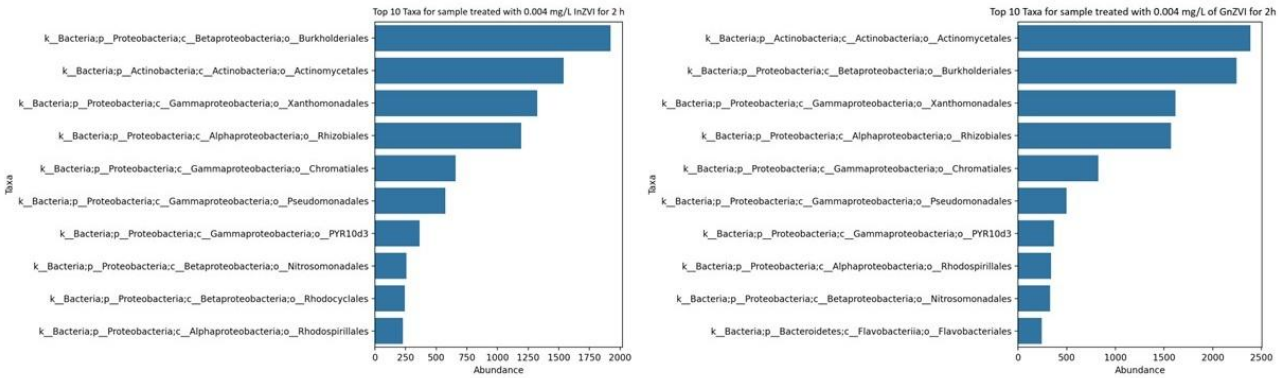


Fig. 2 b: Comparing the abundance of the top 10 bacteria (in OTUs) between samples treated with Industrial and Green nZVI at a dosage of 0.004 mg/L after 2 hours

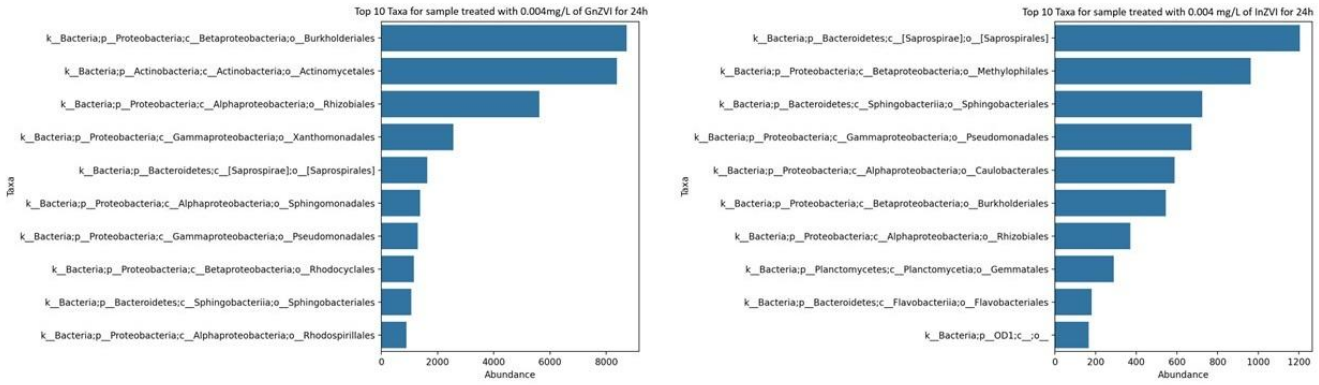


Fig. 2c: Comparing the abundance of the top 10 bacteria (in OTUs) between samples treated with Industrial and Green nZVI at a dosage of 0.004 mg/L after 24 hours

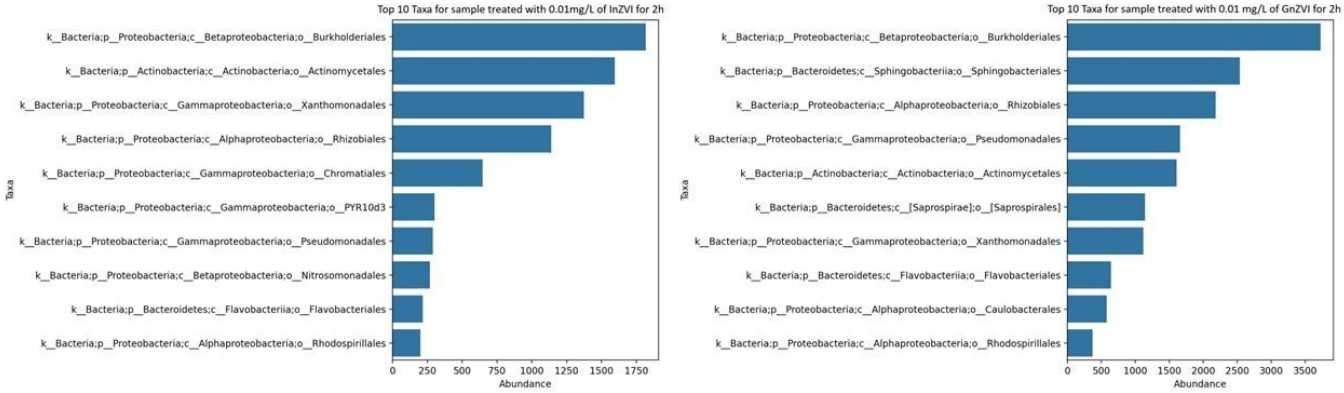


Fig. 2d: Comparing the abundance of the top 10 bacteria (in OTUs) between samples treated with Industrial and Green nZVI at a dosage of 0.01 mg/L after 2 hours

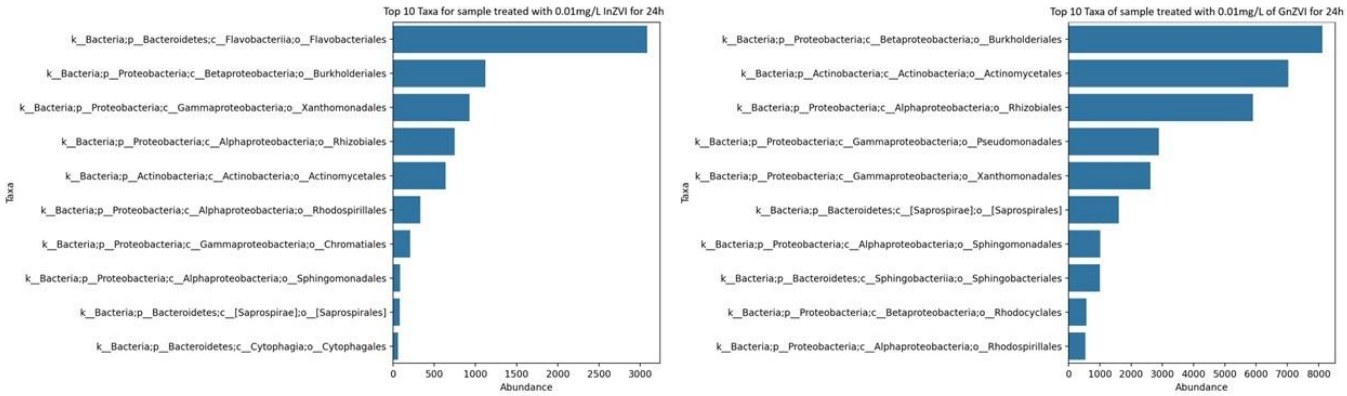


Fig. 2e: Comparing the abundance of the top 10 bacteria (in OTUs) between samples treated with Industrial and Green nZVI at a dosage of 0.01 mg/L after 24 hours

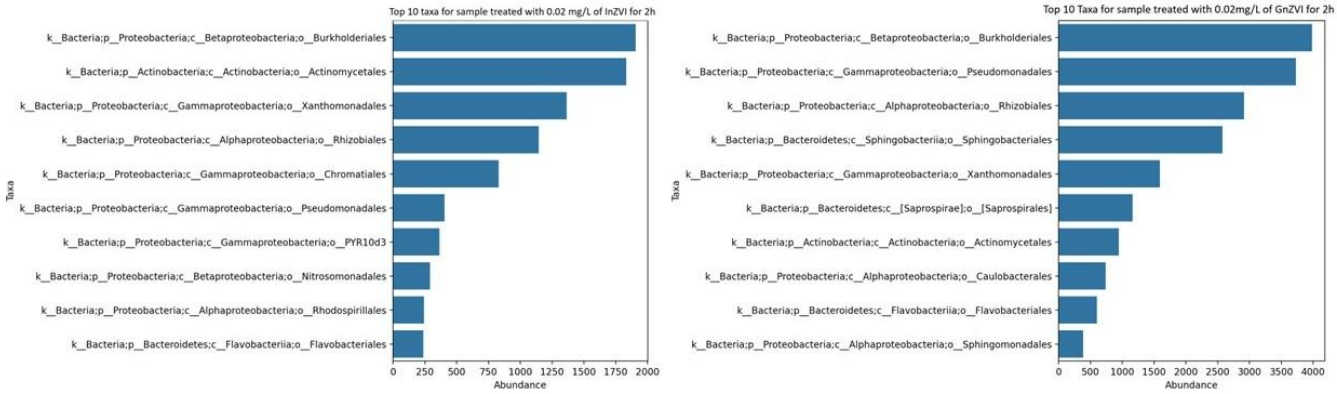


Fig. 2f: Comparing the abundance of the top 10 bacteria (in OTUs) between samples treated with Industrial and Green nZVI at a dosage of 0.02 mg/L after 2 hours.

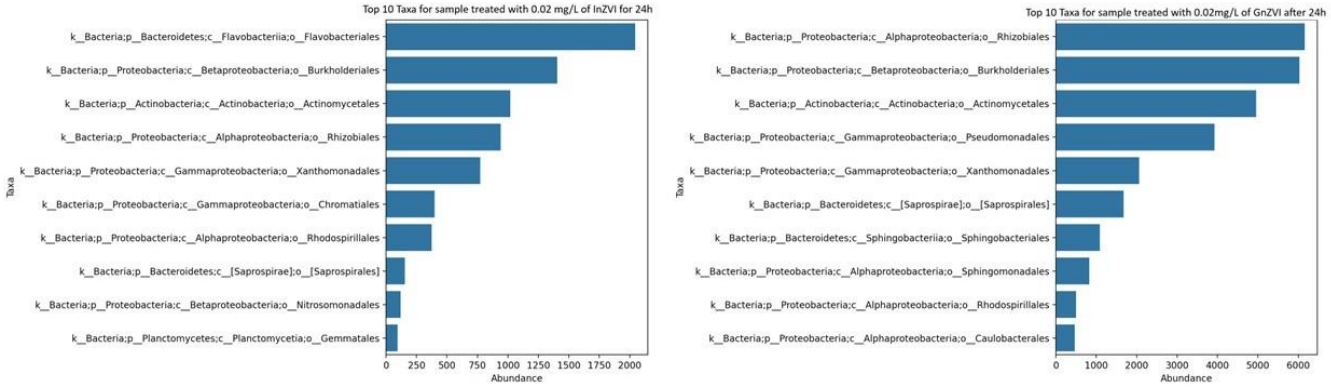


Fig. 2 g: Comparing the abundance of the top 10 bacteria (in OTUs) between samples treated with Industrial and Green nZVI at a dosage of 0.02 mg/L after 24 hours

Figures 2b – 2g present a series of bar charts of the top 10 taxa for each sample, comparing green- and industrial-nZVI treatments (0.004, 0.01, 0.02 mg/L) at two hours and 24 hours against the untreated baseline (Blank CW in Fig. 2a). In the Blank sample, *Flavobacteriia* dominated (2,536 OTUs), followed by *Betaproteobacteria* (1,916), *Alphaproteobacteria* (1,080) and *Actinobacteria* (1,028), reflecting a typical freshwater consortium. Green nZVI drove a pronounced, time-dependent enrichment of hydrocarbon degraders: after 24 hours at 0.004 mg/L, *Betaproteobacteria* increased to 3,306 OTUs, *Gammaproteobacteria* to 2,454 OTUs, while *Flavobacteriia* decreased to 181 OTUs. At 0.02 mg/L dosage after 24 hours, *Actinobacteria* rose to 1,040 OTUs and *Gammaproteobacteria* remained elevated (1,163). In contrast, *Flavobacteriia* dropped further to 107 OTUs, indicating selective promotion of catabolic taxa and suppression of less resilient groups. Industrial nZVI produced sharper but less durable shifts: at 0.02 mg/L dose after 2 hours, *Actinobacteria* peaked at 1,833 OTUs,

and *Flavobacteriia* dropped to 239 OTUs; yet by 24 hours, *Actinobacteria* had fallen to 445 OTUs, and *Gammaproteobacteria* had stabilised at 1,107.

4 Discussion of Results

4.1 Comparing the TPH removal efficiencies of Industrial and Green NZVI

In the blank control, COD fell only slightly from 179mg/l to 172 mg/l within 24 hours, hinting that natural attenuation was negligible. Adding industrial nZVI reduced COD to 112mg/l, 214mg/l and 59 mg/l after two hours at 0.004 mg/L, 0.01 mg/L and 0.02 mg/L, respectively, and by 24 hours, those values plunged to 67mg/l, 22mg/l and 20mg/l, reflecting between 61–88% removal. Green nZVI produced more tempered but still noticeable drops ranging between 24–49% in two hours and 49–68% after 24 hours, with the lowest dose of 0.004 mg/L again outperforming heavier doses. These 50–160 mg/l reductions show that both formulations actively oxidised/reduced organics rather than merely adsorbing them, echoing the COD-to-TPH correlations documented for refinery effluents treated with nZVI in Rasheed et al. (2011).

The GC-FID (Table 3) results revealed that the diesel-range envelope (retention 19–33 min) was greatly diminished after 24 hours. Industrial nZVI lowered TPH from 58 mg/l to 15.7–20.9 mg/l (65–73 % removal), whereas green nZVI achieved 20.9–25.0 mg/l (56–64 %). At two hours, industrial doses broke down 56–67 % of TPH, green only 37–45 %, but the gap narrowed by 24 hours as the green nZVI particles continued to release reactive Fe. Saleh et al. (2025) confirmed comparable convergence, attributing it to slower iron release and reduced oxidative shock in plant-mediated systems.

4.2 Identified Microbial Taxa

The results from the DNA test conducted on the untreated contaminated water sample revealed an oil-typical community, with *Proteobacteria* (64 %), *Bacteroidetes* (18 %) and *Actinobacteria* (14 %) dominating, plus minor *Planctomycetes* and *Verrucomicrobia*. Within these phyla lie specialist hydrocarbonoclastic bacteria (HCB) that exploit alkanes, aromatics or PAHs as sole carbon sources, shaping natural attenuation in petroleum-impacted waters.

At the extremes of salinity and redox potential, two groups prevail. *Halobacteriales* (*Euryarchaeota*) oxidise C_{10}–C_{34} alkanes and low-weight aromatics in hypersaline brines and high-salinity reservoirs (Oren, 2017), while sulfate-reducing Deltaproteobacteria (*Desulfovibrionales*, *Desulfuromonadales*) couple anaerobic alkane/PAH oxidation to sulfate or Fe (III) reduction in anoxic sediments and deep formations. Together, they drive hydrocarbon loss where oxygen is scarce or absent (Davidova et al., 2018, Vigneron et al., 2023).

Aerobic degradation is shared between high-GC (guanine + cytosine content) *Actinomycetales* (*Rhodococcus*, *Mycobacterium*) that attack straight, branched and polycyclic hydrocarbons in soils and sludge, and several Proteobacterial orders (Larkin et al., 1999, Kim et al., 2010). Alphaproteobacterial *Rhodobacterales* and *Sphingomonadales* initiate PAH ring hydroxylation in coastal waters (Kertesz et al., 2017, Le et al., 2014); Betaproteobacterial *Burkholderiales* and *Rhodocyclales* mineralise C_5–C_{16} alkanes and BTEX in groundwater and effluents (Coenye, 2013, Tan and Parales, 2019, Chemerys et al., 2014); Gammaproteobacterial *Pseudomonadales* and *Oceanospirillales* dominate open-ocean spills, rapidly consuming n-alkanes and lighter PAHs (Gutierrez, 2019, Machado et al., 2019). Collectively, these lineages illustrate how hydrocarbon chemistry, salinity, and oxygen regime determine which microbes and enzymatic toolkits drive natural and engineered bioremediation.

4.3 Overall response of the microbial population to nZVI treatment

The summary of total microbial abundance in OTUs presented in Table 4 illustrates how the microbial population reacts to the two iron formulations. Industrial nZVI maintained cell counts close to the blank (approx. 9,200 OTUs) after 2 hours, but all three doses of 0.004, 0.01 and 0.02 mg/L per 100 ml dropped to about 6,500–7,900 OTUs by 24 hours. This reduction is consistent with reports that uncoated nZVI causes short-lived reactive oxygen bursts and transient toxicity (Jang et al., 2014, Lefevre et al., 2016). Green nZVI exhibited the opposite behaviour: populations increased from 9,510 OTUs to roughly 16,900 OTUs at 2 hours and then rose to 34,000–37,000 OTUs at 24 hours, with the lowest dose of 0.004 mg/L yielding the highest biomass (36,900 OTUs). This “sweet-spot” response echoes findings by Castaño et al. (2021). Statistically, the difference between industrial and control was borderline ($t = –2.52$, $p = 0.053$), while green versus control was clearly positive ($t = 3.89$, $p = 0.012$), and green versus industrial was highly significant ($t = –4.15$, $p = 0.002$). Hence, it is safe to conclude that commercial iron acts as a rapid chemical oxidant that suppresses microbes, while green iron sustains abiotic TPH removal while tripling biomass, delivering the nano-bio synergy needed for sustainable remediation.

4.4 Impact of nZVI treatment on specific microbial groups

In the untreated sample with 9,913 OTUs, *Flavobacteriia* dominated (2,536 OTUs, 26.4 %), followed by *Betaproteobacteria* (1,916 OTUs, 19.9 %), *Alphaproteobacteria* (1,080 OTUs, 11.2 %) and *Actinobacteria* (1,028 OTUs, 10.7 %). Green-nZVI shifted this baseline dramatically: after 24 hours at 0.004 mg/L, *Betaproteobacteria* increased to 3,306 OTUs (30.6 % of 10,804 OTUs) and *Gammaproteobacteria* to 2,454 OTUs (22.7 %), while *Flavobacteriia* plummeted to 181 OTUs (1.7 %). At the highest green dose (0.02 mg/L, 24 hours), Actinobacteria surged to 4,953 OTUs (17.9 % of

27,681 OTUs) and *Saprospirae* to 1,674 OTUs (6 %), with *Flavobacteriia* absent. Evidence that polyphenol-capped iron selectively enriches hydrocarbon degraders while suppressing less-tolerant taxa.

Industrial nZVI produced a different pattern: a transient boost at 0.02 mg/L after two hours (Actinobacteria 1,833 OTU, 21.3 % of 8,621 OTU) was followed by a decline at 24 hours (1,020 OTU, 13.3 % of 7,330 OTU); *Flavobacteriia* stayed low and unchanged (approx. 2.8 %). These contrasting trajectories reinforce that green nZVI supports sustained microbial growth and diversity, which are key for nano-bioremediation, while bare industrial particles impose short-lived oxidative stress that can dampen community resilience.

5 Conclusion

5.1 Implications for Sustainable Nanobioremediation

Industrial nZVI behaves like a rapid-fire oxidant as it degrades hydrocarbons swiftly, but its burst of reactive oxygen suppresses biomass, delaying the biological "finishing" step. Green nZVI, coated with polyphenols, releases Fe^{2+}/Fe^{3+} gradually, quenches excess radicals and donates trace organics. At the optimal 0.004 mg/L dose, the microbial community tripled, while 24-hour TPH removal peaked at 64 %. These results prove that high-performance contaminant removal and ecological integrity are compatible goals. By translating fundamental particle surface chemistry into dose windows (low-to-mid green nZVI), contact-time targets, and gene-level checkpoints, this research delivers a practical blueprint for engineers and regulators intent on meeting both remediation and biodiversity mandates. More broadly, it shows how next-generation technologies can weave green synthesis, circular-economy feedstocks and systems-level biological insight into a single, coherent design philosophy.

5.2 Roadmap for Scale-up and Standardisation

Although green nZVI almost matched the performance of industrial particles while tripling microbial abundance, several gaps must be closed before field adoption. Small-scale pilots should test both formulations across contrasting geochemistries (salinity, pH) and extend monitoring beyond 30 days to track iron ageing, aggregation and successive microbial waves. Coupling 16S surveys with functional omics (alkB, pahE, rdhA) will verify that community shifts translate into real metabolic turnover. A cradle-to-grave life-cycle assessment is needed to quantify the energy, solvent and ecotoxicity trade-offs of green versus industrial nZVI, and parallel screening of alternative agro-waste extracts (e.g., fruit peels, spent coffee) could lower costs while avoiding food-chain competition.

To convert laboratory promise into a regulatory standard, the field also needs harmonised standard quality metrics like phenolic titre, Fe^{0} content per litre, allowable zeta-potential and particle-size

ranges, plus step-by-step guidance on dosing, delivery hydraulics and post-treatment monitoring. Embedding such benchmarks in ISO/ASTM methods, national water-quality directives, and corporate sustainability frameworks will give practitioners confidence that bio-based iron can deliver reliable remediation while advancing circular-economy and biodiversity goals.

6 Statements and Declarations

6.1 Funding

The authors declare that no funds, grants, or other support were received during the preparation of this manuscript.

6.2 Ethics and Consent to Participate

Ethics and Consent to Participate declarations: not applicable

6.3 Consent to Publish

Consent to Publish declaration: not applicable.

6.4 Author Contribution Declaration

All laboratory work was designed and performed by Yakubu Yakmut Saleh under the supervision and critical guidance of Dr Charles Knapp, while Akinseye Roland Olanrewaju processed and cleaned the raw DNA data; every author reviewed and approved the final manuscript.

6.5 Competing Interests declaration

The authors declare no competing interests.

6.6 Data Availability Statement

All datasets generated and analysed in this study are publicly available. The DNA Sequencing data and associated metadata have been deposited in the NCBI repository under BioProject ID: PRJNA1354460 and can be accessed using the following link:

https://eur02.safelinks.protection.outlook.com/?url=http%3A%2F%2Fwww.ncbi.nlm.nih.gov%2Fbioproject%2F1354460&data=05%7C02%7Cyakubu.saleh%40strath.ac.uk%7C3f54f36aebf84051feb008de170a0258%7C631e0763153347eba5cd0457bee5944e%7C0%7C0%7C638973528926179336%7CUnknown%7CTWFpbGZsb3d8eyJFbXB0eU1hcGkiOnRydWUsIlYiOiIwLjAuMDAwMCIsIlAiOiJXaW4zMiIsIkFOIjoiTWFpbCIsIldUIjoyfQ%3D%3D%7C0%7C%7C%7C&sdata=%2FcMVLA8v8zckCnSHQC98NqTJn5XQGBRlnsBnS%2Fr7R0c%3D&reserved=0

References

ABBASIAN, F., LOCKINGTON, R., MALLAVARAPU, M. & NAIDU, R. 2015. A Comprehensive Review of Aliphatic Hydrocarbon Biodegradation by Bacteria. *Applied biochemistry and biotechnology,* 176.

ABDEL-SHAFY, H. & MANSOUR, M. 2019. Microbial Degradation of Hydrocarbons in the Environment: An Overview.

ALEGBELEYE, O. O., OPEOLU, B. O. & JACKSON, V. A. 2017. Polycyclic Aromatic Hydrocarbons: A Critical Review of Environmental Occurrence and Bioremediation. *Environmental Management,* 60**,** 758-783.

ALIYAR ZANJANI, M. H., VAFAIE, F., MIRBAGHERI, S. A. & HADIPOUR, V. 2015. Investigation of petroleum-contaminated groundwater remediation using multi-stage pilot system: physical and biological approach. *Desalination and Water Treatment***,** 1-11.

ARUN GAVASKAR, L. T., WENDY CONDIT 2005. COST AND PERFORMANCE REPORT NANOSCALE ZERO-VALENT IRON TECHNOLOGIES FOR SOURCE REMEDIATION *In:* COMMAND, N. F. E. (ed.) *CONTRACT REPORT* ENGINEERING SERVICE CENTER, Port Hueneme, California 93043-4370: BATTELLE.

BANERJEE, M., MUKHERJEE, S. & MUKHERJEE, S. 2022. 7 - Facets of nanoparticle-microbe interactions and their roles in nanobioremediation of environmental pollutants: Biochemical, molecular, and technological perspectives. *In:* IQBAL, H. M. N., BILAL, M. & NGUYEN, T. A. (eds.) *Nano-Bioremediation : Fundamentals and Applications*. Elsevier.

BARZAN, E., MEHRABIAN, S. & IRIAN, S. 2014. Antimicrobial and Genotoxicity Effects of Zero-valent Iron Nanoparticles. *Jundishapur J Microbiol,* 7**,** e10054.

BHAT, M. A., GEDIK, K. & GAGA, E. O. 2023. Chapter 23 - Environmental impacts of nanoparticles: pros, cons, and future prospects. *In:* OZTURK, M., ROY, A., BHAT, R. A., VARDAR-SUKAN, F. & POLICARPO TONELLI, F. M. (eds.) *Synthesis of Bionanomaterials for Biomedical Applications*. Elsevier.

BHATT, P., PANDEY, S. C., JOSHI, S., CHAUDHARY, P., PATHAK, V. M., HUANG, Y., WU, X., ZHOU, Z. & CHEN, S. 2022. Nanobioremediation: A sustainable approach for the removal of toxic pollutants from the environment. *Journal of Hazardous Materials,* 427**,** 128033.

BRADL, H. & XENIDIS, A. 2005. Chapter 3 Remediation techniques. *In:* BRADL, H. B. (ed.) *Interface Science and Technology*. Elsevier.

CAPORASO, J. G., KUCZYNSKI, J., STOMBAUGH, J., BITTINGER, K., BUSHMAN, F. D., COSTELLO, E. K., FIERER, N., PEÑA, A. G., GOODRICH, J. K., GORDON, J. I., HUTTLEY, G. A., KELLEY, S. T., KNIGHTS, D., KOENIG, J. E., LEY, R. E., LOZUPONE, C. A., MCDONALD, D., MUEGGE, B. D., PIRRUNG, M., REEDER, J., SEVINSKY, J. R., TURNBAUGH, P. J., WALTERS, W. A., WIDMANN, J., YATSUNENKO, T., ZANEVELD, J. & KNIGHT, R. 2010. QIIME allows analysis of high-throughput community sequencing data. *Nat Methods,* 7**,** 335-6.

CAPORASO, J. G., LAUBER, C. L., WALTERS, W. A., BERG-LYONS, D., HUNTLEY, J., FIERER, N., OWENS, S. M., BETLEY, J., FRASER, L., BAUER, M., GORMLEY, N., GILBERT, J. A., SMITH, G. & KNIGHT, R. 2012. Ultra-high-throughput microbial community analysis on the Illumina HiSeq and MiSeq platforms. *The ISME Journal,* 6**,** 1621-1624.

CASTAÑO, A., PROSENKOV, A., BARAGAÑO, D., OTAEGUI, N., SASTRE, H., RODRÍGUEZ-VALDÉS, E., GALLEGO, J. L. R. & PELÁEZ, A. I. 2021. Effects of in situ Remediation With Nanoscale Zero Valence Iron on the Physicochemical Conditions and Bacterial Communities of Groundwater Contaminated With Arsenic. *Frontiers in Microbiology,* 12.

CHANG, M. C., SHU, H. Y., HSIEH, W. P. & WANG, M. C. 2005. Using nanoscale zero-valent iron for the remediation of polycyclic aromatic hydrocarbons contaminated soil. *J Air Waste Manag Assoc,* 55**,** 1200-7.

CHEMERYS, A., PELLETIER, E., CRUAUD, C., MARTIN, F., VIOLET, F. & JOUANNEAU, Y. 2014. Characterization of Novel Polycyclic Aromatic Hydrocarbon Dioxygenases from the Bacterial Metagenomic DNA of a Contaminated Soil. *Applied and Environmental Microbiology,* 80**,** 6591-6600.

COENYE, T. 2013. The Family Burkholderiaceae. *The Prokaryotes: Alphaproteobacteria and Betaproteobacteria***,** 759-776.

CRANE, R. A. & SCOTT, T. B. 2012. Nanoscale zero-valent iron: Future prospects for an emerging water treatment technology. *Journal of Hazardous Materials,* 211-212**,** 112-125.

DAVIDOVA, I. A., MARKS, C. R. & SUFLITA, J. M. 2018. Anaerobic Hydrocarbon-Degrading Deltaproteobacteria. *In:* MCGENITY, T. J. (ed.) *Taxonomy, Genomics and Ecophysiology of Hydrocarbon-Degrading Microbes*. Cham: Springer International Publishing.

DEVATHA, C. P., THALLA, A. K. & KATTE, S. Y. 2016. Green synthesis of iron nanoparticles using different leaf extracts for treatment of domestic waste water. *Journal of Cleaner Production,* 139**,** 1425-1435.

DHAKA, A. & CHATTOPADHYAY, P. 2021. A review on physical remediation techniques for treatment of marine oil spills. *Journal of Environmental Management,* 288**,** 112428.

EBRAHIMINEZHAD, A., ZARE-HOSEINABADI, A., SARMAH, A., TAGHIZADEH, S., YOUNES, G. & BERENJIAN, A. 2018. Plant-Mediated Synthesis and Applications of Iron Nanoparticles. *Molecular Biotechnology,* 60.

FAHMY, H., MOHAMED, F., MARZOUQ, M., BAHAA EL-DIN, A., ALSOUDI, A., ASHOOR, O., MOHAMED, M. & MAHMOUD, F. 2018. Review of Green Methods of Iron Nanoparticles Synthesis and Applications. *BioNanoScience,* 8.

GUL, M. Z., RUPULA, K. & RAO, B. S. 2022. Chapter 45 - Nanobioremediation: a novel application of green-nanotechnology in environmental cleanup. *In:* MALIK, J. A. (ed.) *Microbes and Microbial Biotechnology for Green Remediation*. Elsevier.

GUTIERREZ, T. 2019. Marine, Aerobic Hydrocarbon-Degrading Gammaproteobacteria: Overview. *In:* MCGENITY, T. J. (ed.) *Taxonomy, Genomics and Ecophysiology of Hydrocarbon-Degrading Microbes*. Cham: Springer International Publishing.

HAJIPOUR, M. J., FROMM, K. M., AKBAR ASHKARRAN, A., JIMENEZ DE ABERASTURI, D., LARRAMENDI, I. R. D., ROJO, T., SERPOOSHAN, V., PARAK, W. J. & MAHMOUDI, M. 2012. Antibacterial properties of nanoparticles. *Trends in Biotechnology,* 30**,** 499-511.

HAMDY, A., ASKER, M. & ABDELHAMID, S. 2021. Bacteriostatic impact of nanoscale zero-valent iron against pathogenic bacteria in the municipal wastewater. *Biologia,* 76.

JANG, M. H., LIM, M. & HWANG, Y. S. 2014. Potential environmental implications of nanoscale zero-valent iron particles for environmental remediation. *Environ Health Toxicol,* 29**,** e2014022.

KERTESZ, M. A., KAWASAKI, A. & STOLZ, A. 2017. Aerobic Hydrocarbon-Degrading Alphaproteobacteria: Sphingomonadales. *In:* MCGENITY, T. J. (ed.) *Taxonomy, Genomics and Ecophysiology of Hydrocarbon-Degrading Microbes*. Cham: Springer International Publishing.

KHAN, M. A. I., BISWAS, B., SMITH, E., NAIDU, R. & MEGHARAJ, M. 2018. Toxicity assessment of fresh and weathered petroleum hydrocarbons in contaminated soil- a review. *Chemosphere,* 212**,** 755-767.

KIM, S.-J., KWEON, O. & CERNIGLIA, C. E. 2010. Degradation of Polycyclic Aromatic Hydrocarbons by Mycobacterium Strains. *In:* TIMMIS, K. N. (ed.) *Handbook of Hydrocarbon and Lipid Microbiology*. Berlin, Heidelberg: Springer Berlin Heidelberg.

LARKIN, M. J., ALLEN, C. C., KULAKOV, L. A. & LIPSCOMB, D. A. 1999. Purification and characterization of a novel naphthalene dioxygenase from Rhodococcus sp. strain NCIMB12038. *J Bacteriol,* 181**,** 6200-4.

LE, P. T., PONTAROTTI, P. & RAOULT, D. 2014. Alphaproteobacteria species as a source and target of lateral sequence transfers. *Trends in Microbiology,* 22**,** 147-156.

LEFEVRE, E., BOSSA, N., WIESNER, M. R. & GUNSCH, C. K. 2016. A review of the environmental implications of in situ remediation by nanoscale zero valent iron (nZVI): Behavior, transport and impacts on microbial communities. *Sci Total Environ,* 565**,** 889-901.

MACAYA, C. C., DURÁN, R. E., HERNÁNDEZ, L., RODRÍGUEZ-CASTRO, L., BARRA-SANHUEZA, B., DOROCHESI, F. & SEEGER, M. 2019. Bioremediation of Petroleum. *Reference Module in Life Sciences*. Elsevier.

MACHADO, L. F., DE ASSIS LEITE, D. C., DA COSTA RACHID, C. T. C., PAES, J. E., MARTINS, E. F., PEIXOTO, R. S. & ROSADO, A. S. 2019. Tracking Mangrove Oil Bioremediation Approaches and Bacterial Diversity at Different Depths in an in situ Mesocosms System. *Front Microbiol,* 10**,** 2107.

MARTIN, F., MALAGNOUX, L., VIOLET, F., JAKONCIC, J. & JOUANNEAU, Y. 2013. Diversity and catalytic potential of PAH-specific ring-hydroxylating dioxygenases from a hydrocarbon-contaminated soil. *Applied Microbiology and Biotechnology,* 97**,** 5125-5135.

MILLER, J. I., TECHTMANN, S., FORTNEY, J., MAHMOUDI, N., JOYNER, D., LIU, J., OLESEN, S., ALM, E., FERNANDEZ, A., GARDINALI, P., GARAJAYEVA, N., ASKEROV, F. S. & HAZEN, T. C. 2019. Oil Hydrocarbon Degradation by Caspian Sea Microbial Communities. *Front Microbiol,* 10**,** 995.

MIRANDA, M. H., MENEZES, D. B., VEGA-BAUDRIT, J. R., FERREIRA, L. F. R., BHARAGAVA, R. N., IQBAL, H. M. N. & BILAL, M. 2022. 1 - Nanobioremediation: An introduction. *In:* IQBAL, H. M. N., BILAL, M. & NGUYEN, T. A. (eds.) *Nano-Bioremediation : Fundamentals and Applications*. Elsevier.

OLADIPO, A., ALABI, V., MUSE, S., EHIZOJIE, O., SAHEED, E. & OLADOYE, P. O. 2025. 17 - Mycoremediation: A biobased approach toward environmental sustainability. *In:* WU, Q.-S. (ed.) *Management of Mycorrhizal Symbiosis for Mycoremediation and Phytostabilization*. Elsevier.

OREN, A. 2017. Aerobic Hydrocarbon-Degrading Archaea. *In:* MCGENITY, T. J. (ed.) *Taxonomy, Genomics and Ecophysiology of Hydrocarbon-Degrading Microbes*. Cham: Springer International Publishing.

PAISSE, S., GONI, M., STALDER, T., STADLER, T., BUDZINSKI, H. & DURAN, R. 2011. Ring-hydroxylating dioxygenase (RHD) expression in a microbial community during the early response to oil pollution. *FEMS microbiology ecology,* 80**,** 77-86.

PHALE, P. S., BASU, A., MAJHI, P. D., DEVERYSHETTY, J., VAMSEE-KRISHNA, C. & SHRIVASTAVA, R. 2007. Metabolic diversity in bacterial degradation of aromatic compounds. *Omics,* 11**,** 252-79.

RASHEED, Q. J., PANDIAN, K. & MUTHUKUMAR, K. 2011. Treatment of petroleum refinery wastewater by ultrasound-dispersed nanoscale zero-valent iron particles. *Ultrasonics Sonochemistry,* 18**,** 1138-1142.

REBELLO, S., NATHAN, V. K., ANEESH, E. M., SINDHU, R., BINOD, P. & PANDEY, A. 2021. Chapter 37 - Nanoparticles in remediation: strategies and new challenges. *In:* KUMAR, R. P. & BHARATHIRAJA, B. (eds.) *Nanomaterials*. Academic Press.

SALEH, Y. Y., CHARLES, K. & TATYANA, P. 2025. Balancing Efficacy and Sustainability: A Comparative Study of Green-Synthesized and Industrial Nano Zero-Valent Iron for Hydrocarbon remediation. *Next Sustainability*.

TAN, W. A. & PARALES, R. E. 2019. Hydrocarbon Degradation by Betaproteobacteria. *In:* MCGENITY, T. J. (ed.) *Taxonomy, Genomics and Ecophysiology of Hydrocarbon-Degrading Microbes*. Cham: Springer International Publishing.

VIGNERON, A., CRUAUD, P., LOVEJOY, C. & VINCENT, W. F. 2023. Genomic insights into cryptic cycles of microbial hydrocarbon production and degradation in contiguous freshwater and marine microbiomes. *Microbiome,* 11**,** 104.

XU, X., LIU, W., TIAN, S., WANG, W., QI, Q., JIANG, P., GAO, X., LI, F., LI, H. & YU, H. 2018. Petroleum Hydrocarbon-Degrading Bacteria for the Remediation of Oil Pollution Under Aerobic Conditions: A Perspective Analysis. *Front Microbiol,* 9**,** 2885.